Chinese Chemical Letters 35 (2024) 109548

Contents lists available at ScienceDirect

Chinese Chemical Letters

journal homepage: www.elsevier.com/locate/cclet

Organic ferroelastic enantiomers with high T_c and large dielectric switching ratio triggered by order-disorder and displacive phase transition

Zhaohong Chen[1], Mengzhen Li[1], Jinfei Lan, Shengqian Hu, Xiaogang Chen*

Ordered Matter Science Research Center, Nanchang University, Nanchang 330031, China

ARTICLE INFO

Article history:
Received 7 July 2023
Revised 12 January 2024
Accepted 19 January 2024
Available online 23 January 2024

Keywords:
Organic salt
Enantiomers
Ferroelastic
Dielectric switching
Phase transition

ABSTRACT

Molecular-based ferroelastics with dielectric switching properties are highly desirable for their applications on microelectronic dielectric switches, sensors, data storage, and so on. However, the current reports mostly focus on organic-inorganic hybrids containing toxic heavy metal atoms, and the relatively low phase transition temperature limits their application. In this paper, low-toxic organic salt ferroelastic enantiomers (*R*/*S*)-4-fluoro-1-azabicyclo[3.2.1]octonium chloride [(*R*/*S*)-F-321] were designed and synthesized under the introducing chirality strategy. They undergo a 432F422-type ferroelastic phase transition with a high Curie temperature (T_c) of 470 K, simultaneously exhibiting excellent dielectric switching characteristics. In addition to the ordered-disordered movement of cations, the significant displacement of anions is also responsible for such high T_c and large dielectric switching ratios, which is very rare in molecular-based switching materials. This work enriches the development of molecular ferroelastic switching materials and gives inspiration for the exploration of environmentally friendly high T_c organic salt ferroelastics with prominent switching performances.

Ferroelastics are crystals with spontaneous strain as order parameter and their spontaneous strain can be reversed under an external stress field [1–4], which have broad application prospects in mechanical switches, shape memory, energy conversion, information transformation, and storage [5–14]. As one of the three main ferroic materials, ferroelastics have laid the foundation for the research of multiferroics [15–21]. For example, the ferroelastic domain walls of $(C_6H_5C_2H_5NH_3)_2Fe^{II}Cl_4$ crystal act as pinning sites, improving the potential barrier for magnetization reversal and thus achieving force-controlled ferromagnetic switching [16]. Ferroelasticity also allows polarization rotation of multiferroic materials under large stress, thereby giving rise to large piezoelectric response [17,18,21]. Over the years, a large number of inorganic ferroelastic materials have been developed, such as $BaTiO_3$ [22], $BiFeO_3$ [23], and VO_2 [24]. However, these inorganic ferroelastic materials have drawbacks such as containing harmful metals, high energy consumption, or difficulty in regulation, which contradict the concept of green development [25,26]. Therefore, molecular-based ferroelastic materials with advantages such as environmental friendliness, low cost, ease of processing, mechanical flexibility, and structural adjustability show great potential as feasible substitutes for traditional inorganic ferroelastic materials [27–34].

In recent years, molecular-based ferroelastic materials with dielectric switching properties have attracted widespread attention. Many efforts have been made to design and synthesize ferroelastic dielectric switching materials with high phase transition temperatures and large ratios of dielectric switching [35–60]. Currently, most of the reports are mainly on organic-inorganic hybrid perovskite systems, with relatively few simple organic salt systems. Organic-inorganic hybrid perovskites are predominantly composed of toxic metals, posing a potential risk of environmental pollution. In contrast, organic salt molecular materials offer the benefits of low toxicity, cost-effectiveness, lightweight properties, and low acoustic impedance [37,38,44,46,57,61]. Moreover, their exceptional mechanical flexibility has demonstrated advantages in the development of ferroelastic and superelastic materials [62–64]. Furthermore, the current ferroelastic materials rarely achieve the advantages of both high T_c and large dielectric switching ratio, which is not conducive to practical applications. The range of phase transition temperature limits the application of switching materials, while the high T_c characteristic allows materials to operate and work at relatively high or extreme temperatures [65–67]. As a consequence, there is an urgent need to design

* Corresponding author.
E-mail address: chenxg@ncu.edu.cn (X. Chen).
[1] These authors contributed equally to this work.

https://doi.org/10.1016/j.cclet.2024.109548
1001-8417/

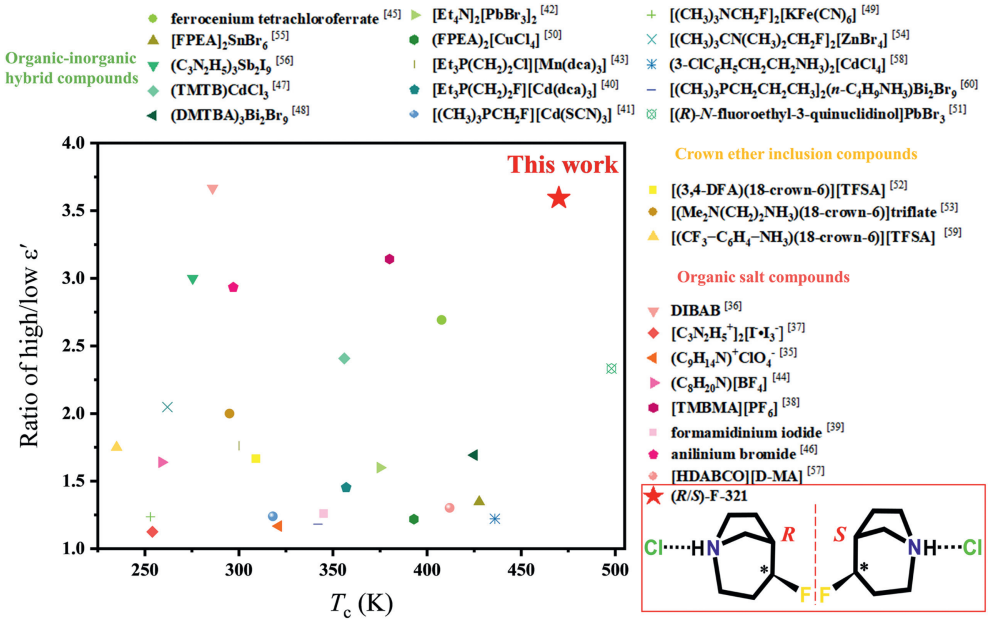

Fig. 1. T_c and the ratio of dielectric switching of (*R*/*S*)-F-321 compared with other compounds at 1 MHz.

and synthesize organic salt ferroelastics with high T_c, which is of great significance for the development of organic salt ferroelastic switching materials.

Recently, Xiong *et al.* proposed the concept of ferroelectrochemistry and elaborated on various targeted chemical design methods for synthesizing molecular ferroelectrics, among which introducing chirality is an effective way to obtain molecular ferroelectrics [66]. This is because chiral materials must crystallize in 11 chiral point groups, 5 of which also are polar point groups, greatly increasing the probability of discovering ferroelectrics [66]. Similarly, according to the 94 species of ferroelastic crystals proposed by Aizu, there are 30 types of chiral-to-chiral ferroelastic phase transition, so introducing chirality also improves the chance of obtaining ferroelastics [1]. Chirality can be generated by the introduction of a fluorine atom into the organic group, and the heavier fluorine atom will increase the potential rotational energy barrier of organic cation, resulting in significant enhancement of T_c [66]. We demonstrated the feasibility of this strategy using organic salt ferroelastic enantiomers (*R*/*S*)-F-321 with high T_c. The chiral organic salt ferroelastics (*R*/*S*)-F-321 crystallize in $P4_32_12$ and $P4_12_12$ chiral space groups at room temperature, respectively, and experience 432F422-type ferroelastic phase transition at 470 K, showing excellent dielectric switching characteristics, which outstrip most molecular-based ferroelastic switching materials (Fig. 1). This work enriches the family of organic salt ferroelastics and switching materials and throws light on the design and synthesis of organic salt ferroelastics with high T_c.

(*R*/*S*)-F-321 were easily obtained as bulk crystals by slow evaporation of the ethanol solution containing equimolar (*R*/*S*)–4-fluoro-1-azabicyclo[3.2.1]octane and hydrochloric acid at 328 K after several days. As shown in Fig. 2a, the DSC curves of (*R*)-F-321 exhibit a pair of thermal anomaly peaks at $T_c = 470$ K (endothermic peak) and 437 K (exothermic peak) with a large thermal hysteresis of 33 K, indicating the first-order phase transition nature. According to the DSC plot, the average enthalpy change (ΔH) is 13.172 kJ/mol, and the average entropy change (ΔS) is 29.063 J mol^{-1} K^{-1}. Based on the Boltzmann equation $\Delta S = R\ln N$ (R is the gas constant, and N is the ratio of the number of independent orientations before and after the phase transition), the value of N is evaluated as 33.026. The large N value means that the (*R*)-F-321 is oriented disorderly in the high-temperature phase. Due to their enantiomeric relationship, (*S*)-F-321 also exhibits similar DSC curves, showing a pair of endothermic/exothermic peaks that appeared at 470 K/437 K (Fig. S1a in Supporting information).

To verify the phase transition behavior of (*R*/*S*)-F-321, we conducted dielectric measurements. As shown in Fig. 2b, the real part (ε') of permittivity at 1 MHz of (*R*)-F-321 shows reversible step-like anomalies around T_c, which accords with the results from DSC measurement. During the heating process, the value of ε' increases slowly from 6.1 at 420 K, then rapidly increases to 23 at 480 K, and finally tends to flatten out after the phase transition. In the cooling process, ε' shows a similar trend, rapidly decreasing from 21.8 at 447 K to 7.5 at 428 K, and then slowing down to 6.9 at 420 K. Below the T_c, the slowly increasing ε' indicates that the dipole motion is frozen, corresponding to the low dielectric state ("Switch OFF"). As the temperature reaches around T_c, the dipole motion is activated and the dielectric constant sharply increases, corresponding to a disordered phase and high dielectric state ("Switch ON"). Similar dielectric anomalies at the phase transition also occur in (*S*)-F-321 (Fig. S1b in Supporting information).

Here, (*R*)-F-321 was selected as a representative for bistable switching measurements at 1 MHz under several sequential cycles to check the stability of switchable dielectric properties. As shown in Fig. 2c, the switching of ε' between the "ON" and "OFF" state is 23 and 6.4 respectively, and the ratio of high and low dielectric states is 3.6. After 11 heating-cooling cycles, the dielectric constant in the "ON" state remained almost unchanged, demonstrating the reversibility and stability. It is rare and commendable that (*R*)-F-321 simultaneously has such a high T_c and a large dielectric switching ratio, which is much better than most molecular dielectric switching materials (Fig. 1). This means that it can still work with high dielectric switching sensitivity in extremely high-temperature environments.

Here, variable-temperature single-crystal X-ray diffractions were carried out to explore the mechanism of the phase transition. At 300 K (RTP), (*R*/*S*)-F-321 crystallizes in the chiral enantiomeric space group $P4_32_12$ and $P4_12_12$ (point group 422) respectively, with the approximate unit cell parameters (Table S1 in Supporting information). As can be seen from Fig. 3a, the asymmetric unit of (*R*/*S*)-F-321 consists of one chiral (*R*/*S*)–4-fluoro-1-

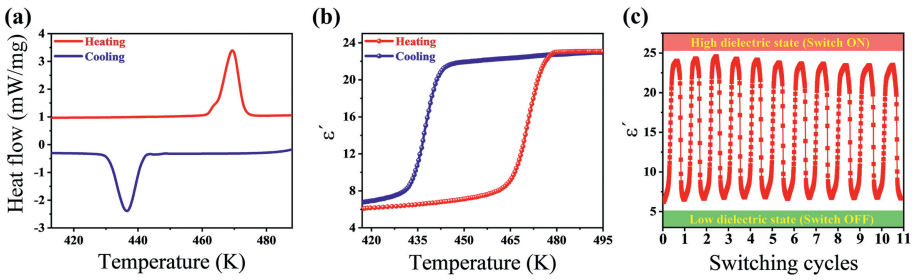

Fig. 2. (a) DSC curves of (*R*)-F-321 in a heating-cooling cycle. (b) Temperature-dependent real part (ε') of the dielectric constant of (*R*)-F-321 at 1 MHz in a heating-cooling cycle. (c) Temperature-driven ε' switching of (*R*)-F-321 at 1 MHz.

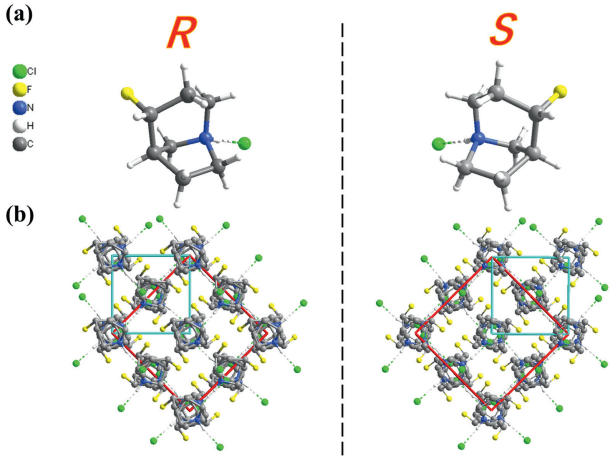

Fig. 3. (a) The asymmetric unit of (*R*/*S*)-F-321 at 300 K. (b) Packing view of (*R*/*S*)-F-321 along the *c*-axis at 300 K (outlined in cyan solid lines representing the RTP cell and outlined in red solid lines representing the HTP cell). The hydrogen atoms are omitted for clarity. The black dashed line denotes a mirror plane.

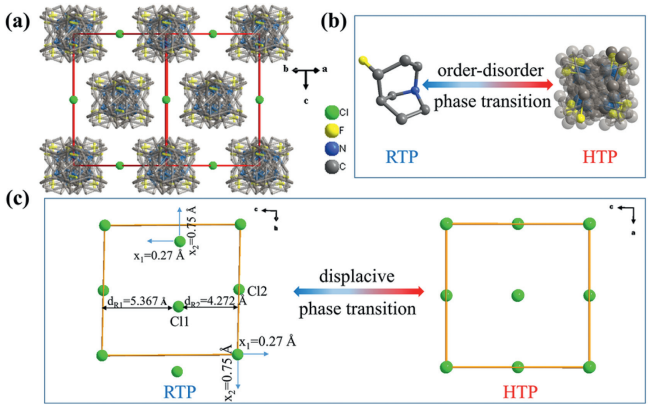

Fig. 4. (a) Packing diagram of (*R*)-F-321 along the *c*-axis at 473 K. (b) Schematic diagram of order-disorder and (c) displacive phase transition mechanism of (*R*)-F-321. The hydrogen atoms are omitted for clarity.

azabicyclo[3.2.1]octonium cation and one chloride anion, where Cl and N atoms are linked by N–H···Cl hydrogen bond with the donor-acceptor distance of 3.0 Å. The N–H···Cl hydrogen bond interaction was also analyzed by using the Hirshfeld surface and 2D fingerprint plot (Fig. S2 in Supporting information) [68]. The red circular depressions on the Hirshfeld dnorm surface and large spikes in the lower left of the fingerprint plot at $d_i \approx 0.7$ Å and $d_e \approx 1.3$ Å highlights the close contact of Cl···H hydrogen bonds. In RTP, the structure is in a completely ordered state, where C, N, and F atoms are wholly distinguishable. The packing view of (*R*/*S*)-F-321 along the *c*-axis at 300 K is shown in Fig. 3b. It can be seen that it is a zero-dimensional packing, with molecules alternately arranged along the 4-fold screw axis, showing the spiral chiral accumulation brought by chiral molecules. Due to their enantiomeric relationship, the structure of (*R*)-F-321 and (*S*)-F-321 display mirror symmetry.

When the temperature increases to 473 K (HTP), (*R*/*S*)-F-321 adopts the same cubic space group *F*432 (point group 432), and the unit cell parameters change significantly with $a=b=c=9.5551(7)$ Å/9.5815(15) Å, $\alpha=\beta=\gamma=90°$, $V=872.38(19)$ Å^3/879.6(4) Å^3, $Z=4$. Compared with the unit cell parameters in RTP, the *a*- and *b*-axes lengths in HTP become longer, the *c*-axis length is greatly shortened, and the cell volume is halved (Fig. 3b and Table S1 in Supporting information). The relation of lattice cells between HTP and RTP is $a^{HTP} \approx \sqrt{2}a^{RTP}$, $b^{HTP} \approx \sqrt{2}b^{RTP}$, and $c^{HTP} \approx 0.25c^{RTP}$. The packing diagram of (*R*)-F-321 in HTP is shown in Fig. 4a. Obviously, compared to the ordered state in RTP, the (*R*)−4-fluoro-1-azabicyclo[3.2.1]octonium cations exhibit a significant orientational motion with 24-fold disorder, showing a nearly symmetric spherical structure in the HTP (Fig. 4b). In addition to the ordered-disordered motion of cations, the remarkable displacement of chloride anions is also responsible for the phase transition. As shown in Fig. 4c, the distances from Cl1 to the left and right planes located in the box in RTP are $d_{R1}=5.367$ Å and $d_{R2}=4.272$ Å, respectively. In order to reach the equilibrium position in HTP, Cl anions in RTP need to move about $x_1=0.27$ Å along the *c*-axis. Moreover, in the *ab* plane, the vertical distance of each chloride ion to the central 4-fold screw axis is $x_2=0.75$ Å, and thus Cl anions in RTP need to move about 0.75 Å to reach the equilibrium position in HTP (Fig. 4c and Fig. S3 in Supporting information). Considering the relatively poor quality of the crystallographic data at 473 K, variable-temperature Powder X-ray Diffraction (PXRD) measurement was performed to further verify the rationality of the high-temperature cubic phase. As shown in Fig. S4a (Supporting information), the significant changes of the peaks within the selected area of the red dashed line demonstrate the structural changes of the (*R*)-F-321. As the temperature increases, the decrease in the number of diffraction peaks indicates that the phase transition is a change from a low-symmetry phase to a high-symmetry phase. The PXRD patterns measured at 297 K and 493 K match very well with the simulated ones, further proving the rationality of the crystallographic data at 300 K and 473 K (Figs. S4b and c). From the foregoing, the displacive changes of chloride anions and order-disorder transition of the 4-fluoro-1-azabicyclo[3.2.1]octonium cations result in the phase transition, leading to ultra-high T_c and large ε' switching.

According to the Aizu rule, (*R*/*S*)-F-321 undergoes a ferroelastic phase transition with an Aizu notation of 432F422. Due to the birefringence characteristics of crystals, ferroelastic domains exhibit bright and dark alternating patterns under orthogonally polarized light. In order to observe the ferroelastic-paraelastic trans-

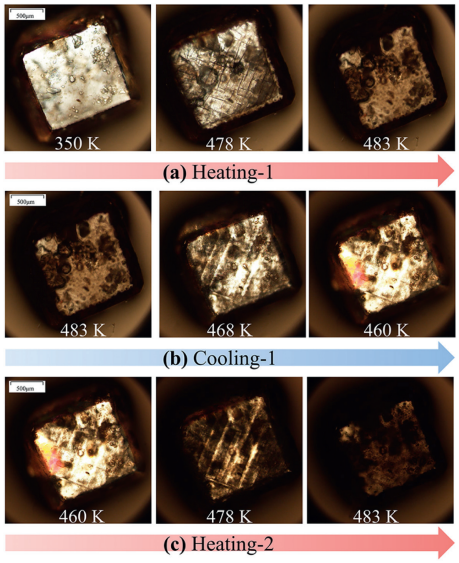

Fig. 5. Evolution of ferroelastic domains between the paraelastic and ferroelastic phase of (*R*)-F-321 in the first heating run (a), the first cooling run (b), and the second heating run (c).

formation of (*R*)-F-321, the single crystal was observed using a polarization microscope during the heating-cooling cycles. As shown in Fig. 5a, no ferroelastic domains were observed in the raw crystal under polarized light at 350 K. When the crystal was heated to 478 K, striped ferroelastic domains with alternating light and dark suddenly appeared. When the temperature rose to 483 K, the crystal underwent a ferroelastic phase transition from the ferroelastic phase to the paraelastic phase, and the domains disappeared completely. Then the crystal was cooled, and as the temperature dropped to 468 K, the streaked ferroelastic domains reappeared, becoming brighter as the temperature decreased (Fig. 5b). After further heating the crystal above T_c, it can be observed that the ferroelastic domains disappeared again (Fig. 5c). The comparison of crystal morphology observed under polarized and depolarized conditions is shown in Fig. S5 (Supporting information), confirming that the existence of ferroelastic domains is independent of morphology. During continuous heating-cooling cycles, the domain structure repeatedly disappeared and appeared, suggesting that the ferroelastic-paraelastic phase transition is reversible.

In summary, we synthesized simple organic salt ferroelastic enantiomers (*R*/*S*)-F-321, which undergo a high-temperature structural phase transition with an Aizu notation of 432F422 at 470 K. Due to the synergistic effect of the order-disorder transition of 4-fluoro-1-azabicyclo[3.2.1]octonium cations and displacive change of chloride anions, (*R*/*S*)-F-321 exhibit outstanding dielectric switching characteristic around T_c, showing good reversibility and stability. Therefore, they become potential candidate materials for switch applications. The organic enantiomers prove that the introduction of chirality is an effective way to develop multifunctional phase transition materials.

Declaration of competing interest

The authors declare that they have no known competing financial interests or personal relationships that could have appeared to influence the work reported in this paper.

Acknowledgment

This work was supported by the National Natural Science Foundation of China (No. 22201120).

Supplementary materials

Supplementary material associated with this article can be found, in the online version, at doi:10.1016/j.cclet.2024.109548.

References

[1] K. Aizu, J. Phys. Soc. Jpn. 27 (1969) 387–396.
[2] J. Sapriel, Phys. Rev. B 12 (1975) 5128–5140.
[3] U. Bismayer, E. Salje, A.M. Glazer, et al., Phase Trans. 6 (1986) 129–151.
[4] S.A.T. Redfern, E. Salje, J. Phys. C: Solid State Phys. 21 (1988) 277–285.
[5] V. Nagarajan, A. Roytburd, A. Stanishevsky, et al., Nat. Mater. 2 (2003) 43–47.
[6] S.H. Baek, H.W. Jang, C.M. Folkman, et al., Nat. Mater. 9 (2010) 309–314.
[7] M. Liu, B.M. Howe, L. Grazulis, et al., Adv. Mater. 25 (2013) 4886–4892.
[8] R. Xu, S. Liu, I. Grinberg, et al., Nat. Mater. 14 (2015) 79–86.
[9] C. Wang, X. Ke, J. Wang, et al., Nat. Commun. 7 (2016) 10636.
[10] X. Lu, Z. Chen, Y. Cao, et al., Nat. Commun. 10 (2019) 3951.
[11] R.G. Xiong, S.Q. Lu, Z.X. Zhang, et al., Angew. Chem. Int. Ed. 59 (2020) 9574–9578.
[12] Y. Hu, L. You, B. Xu, et al., Nat. Mater. 20 (2021) 612–617.
[13] J. Li, Y. Zhu, P.Z. Huang, et al., Chem. Eur. J. 28 (2022) e202201005.
[14] T. Zhang, K. Xu, J. Li, et al., Natl. Sci. Rev. 10 (2023) nwac240.
[15] W.Q. Liao, Y.Y. Tang, P.F. Li, et al., J. Am. Chem. Soc. 139 (2017) 18071–18077.
[16] Y. Nakayama, S. Nishihara, K. Inoue, et al., Angew. Chem. 129 (2017) 9495–9498.
[17] M. Wojciechowska, A. Gągor, A. Piecha-Bisiorek, et al., Chem. Mater. 30 (2018) 4597–4608.
[18] C. Shi, J.J. Ma, J.Y. Jiang, et al., J. Am. Chem. Soc. 142 (2020) 9634–9641.
[19] Z.X. Wang, X.G. Chen, X.J. Song, et al., Nat. Commun. 13 (2022) 2379.
[20] Y.L. Zeng, Y. Ai, S.Y. Tang, et al., J. Am. Chem. Soc. 144 (2022) 19559–19566.
[21] X.G. Chen, Y.Y. Tang, H.P. Lv, et al., J. Am. Chem. Soc. 145 (2023) 1936–1944.
[22] X. Moya, E. Stern-Taulats, S. Crossley, et al., Adv. Mater. 25 (2013) 1360–1365.
[23] A. Bhatnagar, A.Roy Chaudhuri, Y.Heon Kim, et al., Nat. Commun. 4 (2013) 2835.
[24] Q. WY, J. ZZ, et al., ACS Nano 2 (2008) 1492–1496.
[25] G.H. Haertling, J. Am. Ceram. Soc. 82 (1999) 797–818.
[26] D.J. Goossens, Acc. Chem. Res. 46 (2013) 2597–2606.
[27] D.W. Fu, H.L. Cai, Y. Liu, et al., Science 339 (2013) 425–428.
[28] S. Chen, R. Shang, B.W. Wang, et al., Angew. Chem. Int. Ed. 54 (2015) 11093–11096.
[29] P.P. Shi, Y.Y. Tang, P.F. Li, et al., J. Am. Chem. Soc. 139 (2017) 1319–1324.
[30] Z. Sun, X. Yi, K. Tao, et al., Angew. Chem. Int. Ed. 57 (2018) 9833–9837.
[31] H.Y. Zhang, Y.Y. Tang, P.P. Shi, et al., Acc. Chem. Res. 52 (2019) 1928–1938.
[32] J. Long, M.S. Ivanov, V.A. Khomchenko, et al., Science 367 (2020) 671–676.
[33] Y.L. Zeng, X.Q. Huang, C.R. Huang, et al., Angew. Chem. Int. Ed. 60 (2021) 10730–10735.
[34] P.F. Li, Y. Ai, Y.L. Zeng, et al., Chem. Sci. 13 (2022) 657–664.
[35] Y. Zhang, K. Awaga, H. Yoshikawa, et al., J. Mater. Chem. 22 (2012) 9841–9845.
[36] A. Piecha-Bisiorek, A. Bialoska, R. Jakubas, et al., Adv. Mater. 27 (2015) 5023–5027.
[37] M. Weclawik, P. Szklarz, W. Medycki, et al., Dalton Trans. 44 (2015) 18447–18458.
[38] X.G. Chen, J.X. Gao, X.N. Hua, et al., New J. Chem. 42 (2018) 14909–14913.
[39] K. Mencel, P. Durlak, M. Rok, et al., RSC Adv. 8 (2018) 26506–26516.
[40] M.M. Zhao, L. Zhou, P.P. Shi, et al., Chem. Commun. 54 (2018) 13275–13278.
[41] Y.J. Cao, L. Zhou, P.P. Shi, et al., Chem. Commun. 55 (2019) 8418–8421.
[42] Y. Huang, J. Yang, Z.J. Li, et al., RSC Adv. 9 (2019) 10364–10370.
[43] M.M. Zhao, L. Zhou, P.P. Shi, et al., Chem. Eur. J. 25 (2019) 6447–6454.
[44] M. Moskwa, E. Ganczar, P. Sobieszczyk, et al., J. Phys. Chem. C 124 (2020) 18209–18218.
[45] H.Y. Zhang, C.L. Hu, Z.B. Hu, et al., J. Am. Chem. Soc. 142 (2020) 3240–3245.
[46] D.W. Fu, J.X. Gao, P.Z. Huang, et al., Angew. Chem. Int. Ed. 60 (2021) 8198–8202.
[47] X.Q. Xu, H. Zhang, X.Q. Huang, et al., Inorg. Chem. Front. 8 (2021) 1197–1204.
[48] Z.X. Zhang, C.Y. Su, J. Li, et al., Chem. Mater. 33 (2021) 5790–5799.
[49] X.G. Chen, Z.X. Zhang, Y.L. Zeng, et al., Chem. Commun. 58 (2022) 3059–3062.
[50] Y.P. Gong, X.X. Chen, G.Z. Huang, et al., J. Mater. Chem. C 10 (2022) 5482–5488.
[51] Y.Y. He, Z. Chen, X.G. Chen, et al., Mater. Chem. Front. 6 (2022) 1292–1300.
[52] J.C. Liu, F.F. Di, Y.P. Zeng, et al., Inorg. Chem. Front. 9 (2022) 5799–5804.
[53] M.M. Lun, T. Zhang, C.Y. Su, et al., Mater. Chem. Front. 6 (2022) 1929–1937.
[54] X. Meng, Z.B. Liu, K. Xu, et al., Inorg. Chem. Front. 9 (2022) 1603–1608.
[55] T. Shao, H.F. Ni, C.Y. Su, et al., Chem. Eur. J. 28 (2022) e202202533.
[56] P. Szklarz, R. Jakubas, W. Medycki, et al., Dalton Trans. 51 (2022) 1850–1860.
[57] N. Zhang, Y. Zhang, H.H. Jiang, et al., Chem. Mater. 34 (2022) 8077–8086.
[58] Y.P. Gong, X.X. Chen, B.Q. Zhao, et al., Chin. Chem. Lett. 34 (2023) 108282.
[59] H.P. Lv, Y.R. Li, X.J. Song, et al., J. Am. Chem. Soc. 145 (2023) 3187–3195.
[60] J. Mu, K. Xu, L. He, et al., Chem. Commun. 59 (2023) 1209–1212.
[61] W.Q. Liao, Y.L. Zeng, Y.Y. Tang, et al., J. Am. Chem. Soc. 143 (2021) 21685–21693.
[62] S. Sakamoto, T. Sasaki, A. Sato-Tomita, et al., Angew. Chem. Int. Ed. 58 (2019) 13722–13726.

[63] T. Sasaki, S. Sakamoto, Y. Takasaki, et al., Angew. Chem. Int. Ed. 59 (2020) 4340–4343.
[64] Y.X. Li, Z.K. Liu, J. Cao, et al., Angew. Chem. Int. Ed. 62 (2023) e202217977.
[65] D.W. Fu, J.X. Gao, W.H. He, et al., Angew. Chem. Int. Ed. 59 (2020) 17477–17481.
[66] H.Y. Liu, H.Y. Zhang, X.G. Chen, et al., J. Am. Chem. Soc. 142 (2020) 15205–15218.
[67] X. Mu, L. Xu, Y.Y. Xu, et al., Mater. Chem. Front. 5 (2021) 8371–8379.
[68] P.R. Spackman, M.J. Turner, J.J. McKinnon, et al., J. Appl. Cryst. 54 (2021) 1006–1011.